H$_2$O speciation in float glass and soda lime silica glass

A. Stuke [a,1], H. Behrens [a,*], B.C. Schmidt [b,2], R. Dupree [c]

[a] *Institut für Mineralogie, Universität Hannover, Callinstrasse 3, D-30167 Hannover, Germany*
[b] *Bayerisches Geoinstitut, Universität Bayreuth, D-95440 Bayreuth, Germany*
[c] *Department of Physics, University of Warwick, Coventry, CV4 7AL, United Kingdom*

Abstract

The speciation of H$_2$O in float glass (FG) and soda lime silica glass (SLS) was investigated using IR and NMR spectroscopy. Molar absorption coefficients for the near-infrared (NIR) combination bands at 4500 and 5200 cm^{-1}, assigned to OH groups and H$_2$O molecules, respectively, were determined using hydrated glasses containing 0.5–7.4 wt.% of dissolved H$_2$O. Water contents of the samples used in the calibration were determined by Karl–Fischer titration or mid-infrared spectroscopy. Different combinations of baseline corrections and intensity measures were applied to evaluate the NIR spectra with tangent baselines and measurement of peak heights giving the best reproducibility. Deviations up to 30% relative were observed between water species concentrations determined by NIR spectroscopy using an internally consistent calibration based on bulk water content and those determined by low temperature static ^{1}H NMR spectroscopy. This implies that the assumption of constant NIR absorption coefficients may be not valid for glasses in which dissolved water is strongly hydrogen-bonded. Based on the NMR data the NIR absorption coefficients were re-calibrated, demonstrating that in particular the absorption coefficient for the band at 4500 cm^{-1} (ε_{4500}) varies with water content. For float glass ε_{4500} grows by 35% when the water content increases from 0.5 to 4.0 wt.%. An opposite trend was found for soda lime glass with an approximately linear decrease of ε_{4500} by 27% relative between 0.5 and 7.5 wt.% H$_2$O. For the 5200 cm^{-1} band we could not resolve a dependence of the absorption coefficient (ε_{5200}) on water content (values of 0.89±0.06 and 0.95±0.06 L mol^{-1} cm^{-1} were determined for FG and SLS glass, respectively). However, this may be a consequence of the low precision in determining of ε_{5200} at water contents below 2 wt.%. Based on the improved NIR calibrations, the OH concentrations at given water content are typically lower in FG than in SLS glasses with apparent saturation values of 1.4 wt.% (FG) and 2.2 wt.% (SLS) of water dissolved as OH groups. The difference in OH contents could be related to the different chemical compositions of these two glasses, in particular the concentration of alkaline-earth elements and the ratio of Mg/Ca, which are larger in FG glass than in SLS glass. Using the new water speciation data, we have re-evaluated the molar absorption coefficient for the H$_2$O bending vibration band at 1630 cm^{-1}.

* Corresponding author. Tel.: +49 511 762 8054; fax: +49 511 762 3045.
 E-mail address: h.behrens@mineralogie.uni-hannover.de (H. Behrens).
[1] Present address: Forschungszentrum Jülich, Institut für Werkstoffe und Verfahren der, Energietechnik, D-52425 Jülich.
[2] Present address: GZG, Georg-August Universität Göttingen, Goldschmidtstr. 1, D-37077, Göttingen, Germany.

1. Introduction

Infrared spectroscopy is a well established technique to quantify dissolved water in industrial and natural glasses. As shown by near-infrared (NIR) and nuclear magnetic resonance (NMR) spectroscopy, water dissolves in silicate glasses as OH groups and H_2O molecules (Scholze, 1960; Bartholomew and Schreurs, 1980; Stolper, 1982a,b; Eckert et al., 1988; Schmidt et al., 2001). In silicate glasses OH groups are usually bonded to silicon (Kohn et al., 1989; Zotov and Keppler, 1998; Robert et al., 2001), but recent NMR findings give evidence that additionally free OH– ions are linked to Mg and Ca in alkaline earth silicates (Xue and Kanzaki, 2004). In aluminosilicate glasses OH groups may also form bridges between two tetrahedral cations (Kohn et al., 1989). The interconversion of OH groups and H_2O molecules can be described with the reaction

$$H_2O + O \Leftrightarrow 2OH \qquad (1)$$

where O is an anhydrous oxygen. Assuming ideal mixing of the H_2O, O and OH, the equilibrium constant K_{ws} for reaction (1) is given by

$$K_{ws} = \frac{[OH]^2}{[H_2O] \cdot [O]} \qquad (2)$$

where square brackets refer to mole fractions calculated on a single oxygen basis. At low water contents, which are typically found in technical glasses, OH groups are predominant and molecular H_2O concentration is often below the detection limit. With increasing water content the relative abundance of H_2O molecules grows and it becomes the dominant species above 3–6 wt.% H_2O_t (hereafter the term H_2O_t is used for the total water content whereas H_2O refers to water incorporated in molecular form), depending on glass composition and cooling rate (Silver et al., 1990; Behrens et al., 1996; Zhang et al., 1997; Behrens and Nowak, 2003).

The hydrous species are assumed to have different effects on the structure and properties of silicate glasses and melts. The formation of OH groups results in depolymerization and weakening of the silicate network (Scholze, 1960; Stolper, 1982a,b; Kohn et al., 1989). As a consequence, the viscosity of melts is strongly reduced (Persikov et al., 1990; Hess and Dingwell, 1996; Richet et al., 1996; Schulze et al., 1996; Romano et al., 2001; Giordano and Dingwell, 2003; Giordano et al., 2004; Whittington et al., 2004) and the diffusivity of melt components is strongly enhanced (Baker, 1991; Watson, 1994; Koepke and Behrens, 2001). Additionally, the electrical conductivity of the glasses may increase due to

contributions of proton hopping from OH groups to neighboring non-bridging oxygen (Behrens et al., 2002). H_2O molecules, on the other hand, play an important role in water diffusion and degassing of silicate melts (Zhang et al., 1991; Watson, 1994).

Specific absorption bands for OH groups and H_2O molecules are observed in the near-infrared domain at ~4500 and ~5200 cm^{-1}, respectively, which can be used for quantitative determination of species concentrations (Scholze, 1960; Bartholomew et al., 1980; Stolper, 1982a,b). Knowledge of the density of the sample and the molar absorption coefficient is required for the evaluation of the near-infrared spectra. These properties strongly depend on anhydrous glass composition (Silver et al., 1990; Behrens et al., 1996; Richet et al., 2000; Ohlhorst et al., 2001).

Most of previous NIR spectroscopic studies were focused on aluminosilicate glasses with weak or negligible hydrogen bonding as indicated by the simple asymmetric OH stretching vibration band near 3500 cm^{-1} (Stolper, 1982a,b; Silver et al., 1990; Dixon et al., 1995; Behrens et al., 1996; Zhang et al., 1997; Withers and Behrens, 1999; Yamashita et al., 1999; Ohlhorst et al., 2001; Schmidt et al., 2001; Mandeville et al., 2002). For these glasses it has been generally assumed that the absorption coefficients for the NIR bands are independent of water content. Support for this assumption is given by the good agreement between NIR and static ^1H NMR spectroscopic determinations of hydrous species in various alkali aluminosilicates (Schmidt et al., 2001). However, the assumption of constant absorption coefficients may not be generally valid. Zhang et al. (1997) found indications of the variation of absorption coefficients with water content for hydrous rhyolitic glasses with water contents below 2.4 wt.%. A general trend of an increasing absorption coefficient for the 4500 cm^{-1} band with increasing water content was observed by Peuker et al. (2003) for various silicate and aluminosilicate glasses, including several glasses with pronounced hydrogen bonding.

The observed differences in variation of absorption coefficients with water content may be related to the ranges of water content used in the studies (variations have been observed at relatively low water contents) and the procedures used for spectra evaluation. A general problem is that an independent confirmation of species concentration by another method is often missing and absorption coefficients are based only on an internally consistent calibration using bulk water determinations.

Here we present a systematic calibration of molar absorption coefficients for the NIR bands of hydrous species in float glass and soda lime silica glass. A large

range of water contents from 0.52 to 7.42 wt.% was used to investigate possible variations of the absorption coefficients. Static ^1H NMR measurements were performed on selected samples to verify the species concentrations and to optimize the NIR calibration. Different procedures for evaluation of the NIR bands were tested with respect to accuracy and reproducibility of the determination of concentrations of hydrous species.

2. Synthesis and analytical methods

2.1. Starting materials

As anhydrous starting materials a float glass (FG) synthesized by Potters–Ballotini Company and a soda lime silicate glass (SLS) synthesized by Schott company were used. An additional soda lime silicate glass (SLSa) was synthesized by melting a mixture of carbonates and oxides in a platinum crucible for 4 h at 1500 °C s. Glass compositions were analyzed with a Cameca SX100 electron microprobe (Table 1).

2.2. Hydrous glasses

Most of the glasses were already used in a study on mid-infrared spectroscopy (Behrens and Stuke, 2003). Hydrous glasses were produced by fusion of anhydrous glass powder and defined amounts of water in a platinum capsule at high temperature and pressure. In order to homogenize glass pieces, glass powder and water were filled in several portions into platinum

capsules (diameter: 4–6 mm length: 25–40 mm) before sealing by arc welding. Capsules were checked for possible leakage by testing the weight loss after drying at 380 K for several hours.

All syntheses were performed in an internally heated gas pressure vessel (IHPV) at temperatures in the range of 1473–1523 K and pressures between 100 and 500 MPa. Samples were quenched with an initial rate of 200 K/min by switching off the furnace power. The cooling rate decreases with temperature to about 100K/min in the range of glass transition (523–773 K for our glasses). To study the effect of quench rate, one FG and one SLS glass (FG-5ASASQ and SLSa-A4SQ) were cooled at a much slower rate through the range of the glass transition in which water speciation is frozen in (rapid cooling with 100 K/min from 1523 to 823 K and then slow cooling with 5 K/min to room temperature).

Water contents of most of the glasses were determined by Karl–Fischer-Titration (KFT) after thermal dehydration of glass wafers or by mid-infrared spectroscopy (Behrens and Stuke, 2003). To account for unextracted water (Behrens and Stuke, 2003), water contents measured by KFT were corrected by adding 0.13 wt.% H_2O_t.

2.3. IR Spectroscopy

Doubly polished glass plates with thicknesses in the range of 0.3–1.7 (±0.02) mm were prepared for near-infrared spectroscopy. Absorption spectra in the range 2000–10000 cm^{-1} were measured with a Bruker IFS88 FTIR spectrometer using a tungsten

Table 1
Compositions of glasses

	SLS	SLSa	FG
	Wt.% oxides		
SiO_2	73.59 (±0.49)	73.29 (±0.70)	72.01 (±0.55)
Al_2O_3	0.02 (±0.04)	0.04 (±0.04)	0.76 (±0.06)
Fe_2O_3	0.02 (±0.09)	0.00 (±0.08)	0.10 (±0.09)
MgO	0.00 (±0.00)	0.00 (±0.00)	3.92 (±0.12)
CaO	9.32 (±0.23)	9.39 (±0.23)	8.96 (±0.18)
Na_2O	15.83 (±0.31)	16.08 (±0.57)	13.13 (±0.28)
K_2O	0.02 (±0.01)	0.01 (±0.01)	0.25 (±0.05)
H_2O*	0.030	0.012	0.045
Total	98.80	98.78	99.20
NBO/T	0.69	0.70	0.77
Cation fraction of $Al^{3+}+Si^{4+}$	0.64	0.64	0.64

Each analysis is based on 10 measurements using an electron microprobe CAMECA SX100 (conditions: 15 kV acceleration voltage, 6 nA beam current, electron beam defocused to 15 µm diameter). 1 σ errors are given in parenthesis.
*The H_2O content was determined from the peak height of the IR absorption band at 2850 cm^{-1} using the absorption coefficients obtained in Behrens and Stuke (2003).

lamp as light source and a CaF_2 beam splitter. Spectral resolution was 4 cm^{-1} and 50–100 scans were accumulated for each spectrum. Most of the spectra were recorded using an IR scope II microscope equipped with a narrow range MCT detector. A slit aperture between the objective and the detector was used to limit the sample volume analyzed. In the focus plane, the area selected by the slit was typically $100 \cdot 100$ μm^2. Bulk spectra of glasses with sizes larger than 2 mm diameter were measured in the main chamber of the spectrometer using an InSb detector. Consistency of both measurements was tested for several glasses. Deviation in absorbance after baseline subtraction was always within ±0.003.

2.4. NMR Spectroscopy

Static ^1H NMR spectra of two glasses (SLS-7NMR, FG-4NMR) were acquired at 140 K at Warwick University using a Chemagnetics® Infinity 360 (B_0=8.45 T) and a Bruker® static ^1H-probe with a low proton background and a short dead time (3 μs). Samples were glass cylinders typically 200–400 mg in weight. In order to account for a small proton signal from the NMR probe, the sample spectra were background corrected by collecting ^1H NMR free induction decays (FID) of the probe (without sample) with exactly the same acquisition parameters as used for the glasses. These were then subtracted from the sample FID. Details of the NMR measurements are reported by Schmidt et al. (2001).

3. Results

3.1. IR Spectroscopy

Fig. 1A and B show selected near-infrared spectra of soda lime silica glass (a) and float glass (b) with typical absorption bands in the range of 4000–8000 cm^{-1}. The 4500 cm^{-1} band is assigned to the combination of stretching and bending of structurally bonded OH groups, and the band at 5200 cm^{-1} to the combination of stretching and bending modes of H_2O molecules (Scholze, 1960; Bartholomew et al., 1980; Stolper, 1982a,b). The band at 7000 cm^{-1} is attributed to the first overtone of the OH stretching vibration of OH groups and H_2O molecules (at 3500 cm^{-1}) (Stolper, 1982a,b). Superimposed to the NIR combination and overtone bands is the long tail of the OH stretching vibration band extending beyond 8000 cm^{-1}.

With increasing water content the band at 5200 cm^{-1} strongly grows whereas little change is observed in the
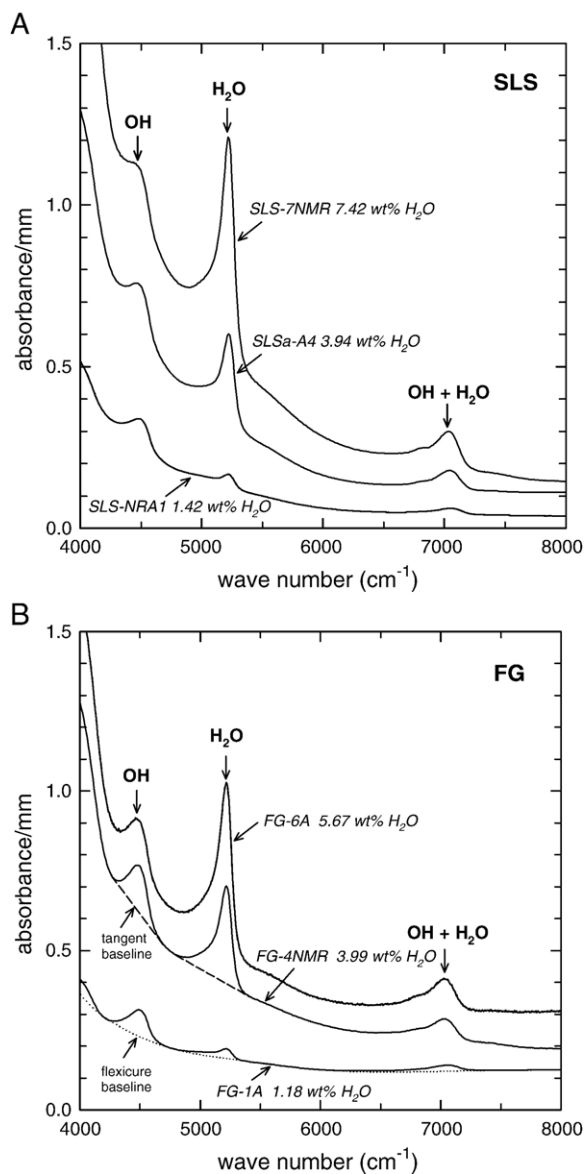

Fig. 1. Near-infrared absorption spectra of soda-lime silica glass (A) and float glass (B). Spectra are plotted with an offset for clarity. The tangential-baseline is shown as dashed line and the flexi curve baseline is illustrated dotted in (B).

intensity of the 4500 cm^{-1} band for water contents above 2 wt.%. For quantitative evaluations of the bands intensities, a baseline correction was applied using either a flexi curve (FC) or tangents (TT) (Withers and Behrens, 1999). Both types of baselines are illustrated as examples in Fig. 1B for FG glass. The band intensities for TT and FC baselines and peak areas for FC baseline are presented in Table 2.

FC-baseline-corrected spectra of float glass are shown in Fig. 2A and B. With increasing water content

Table 2
Sample description and spectroscopic data

Sample	$C_{H_2O_t}$ (wt.%)	$C_{H_2O_t}$ (mol/L)	Density (g/l)	Thickness (cm)	A_{4500}	$A_{4500}*$ (cm⁻¹) FC baseline	A_{5200}	$A_{5200}*$ (cm⁻¹)	A_{4500} TT baseline	A_{5200} TT baseline	C_{OH} (wt.%) TT baseline	C_{H_2O} (wt.%)
SLS-NRA2	0.51[§]	0.71	2498	0.0926	0.031	5.9	0.008	4.2	0.030	0.002	0.45	0.02
SLSaA0-5	0.55	0.76	2497	0.0496	0.023	3.9	0.004	1.0	0.020	0.003	0.54	0.04
SLSa1A	0.78	1.08	2494	0.0496	0.030	6.3	0.009	2.4	0.026	0.006	0.72	0.09
SLS-NRA1	1.42[§]	1.96	2484	0.0927	0.053	14.9	0.006	13.3	0.070	0.032	1.08	0.27
SLS2A	1.91[§]	2.63	2477	0.0492	0.055	11.1	0.039	7.4	0.047	0.037	1.38	0.57
SLS3A	2.74	3.75	2465	0.0493	0.067	15.5	0.078	15.7	0.052	0.074	1.62	1.16
SLSa3A	2.92	3.99	2462	0.0501	0.075	13.9	0.084	15.5	0.055	0.077	1.69	1.18
SLS4A	3.75	5.10	2450	0.0489	0.086	18.2	0.134	22.1	0.059	0.131	1.93	2.07
SLSa4A	3.95	5.37	2447	0.0500	0.082	17.1	0.140	24.5	0.060	0.136	1.94	2.10
SLSa4A-SQ[b]	3.95	5.37	2447	0.0486	0.065	n.d.	0.144	n.d.	0.052	0.140	1.75	2.23
FG0-25D[a,b]	0.53[§]	0.73	2486	0.1746	0.068	14.0	0.008	2.3	0.064	0.006	0.50	0.03
FG0-25A[a,b]	0.61[§]	0.85	2497	0.1739	0.079	15.8	0.012	3.6	0.073	0.009	0.58	0.04
FG0-25B[a]	0.61	0.85	2501	0.1747	0.081	16.6	0.011	2.7	0.074	0.009	0.58	0.04
FG0-5-Z	0.71[§]	0.98	2492	0.0979	0.053	10.3	0.013	2.7	0.047	0.009	0.65	0.07
FG0-75E[a]	0.96	1.32	2484	0.1728	0.126	26.7	0.034	8.2	0.110	0.030	0.85	0.14
FG1A[b]	1.18[§]	1.63	2488	0.0982	0.083	16.4	0.031	5.9	0.075	0.029	0.99	0.24
FG1A[a,b]	1.18[§]	1.63	2488	0.1742	0.148	29.6	0.053	10.3	0.134	0.051	1.00	0.24
FG2AI	2.21	3.04	2481	0.0990	0.133	26.5	0.113	19.7	0.111	0.109	1.34	0.90
FG2AII[a]	2.32	3.20	2481	0.1565	0.214	43.2	0.184	33.4	0.184	0.177	1.39	0.92
FG2AII	2.32	3.20	2481	0.0980	0.134	26.0	0.112	17.9	0.113	0.111	1.36	0.92
FG3AI	3.20[§]	4.76	2491	0.0520	0.093	19.6	0.116	19.4	0.067	0.113	1.41	1.77
FG3AII	3.34[§]	4.74	2491	0.0514	0.092	19.2	0.120	21.2	0.068	0.113	1.43	1.79
FG4N[b]	3.92[§]	5.37	2469	0.0304	0.056	11.7	0.098	17.4	0.042	0.094	1.44	2.54
FG4A	4.20	5.79	2484	0.0518	0.107	22.9	0.169	28.6	0.072	0.167	1.42	2.63
FG5BAS[b]	4.55	6.13	2428	0.0332	0.061	12.6	0.145	25.6	0.043	0.138	1.32	3.48
FG4AS[a,b]	4.92[§]	6.68	2445	0.0425	0.093	20.4	0.184	31.3	0.064	0.183	1.47	3.56
FG5ASA[b]	5.23[§]	7.08	2439	0.0425	0.104	23.2	0.205	34.6	0.065	0.203	1.47	3.97
FG5ASA-SQ[b]	5.23	7.08	2439	0.0482	0.079	n.d.	0.249	n.d.	0.069	0.225	1.37	3.87
FG6AS[b]	5.67	7.63	2426	0.0325	0.066	13.2	0.171	29.3	0.045	0.170	1.31	4.35.3

A=absorbance, $A*$=integrated intensity. Abbreviation SQ in the sample name refers to slow quench experiments (5 K/ min). $C_{H_2O_t}$ was determined by mid-infrared spectroscopy using the peak height of the 2850 cm⁻¹ (Behrens and Stuke, 2003) except for samples characterized by [§] for which Karl–Fischer titration was used. $C_{H_2O_t}$ is converted from wt.% to mol/L by multiplying with density/(100 molar mass of H₂O). Density of hydrous soda lime silica glass and float glass is calculated as $\rho=2505-14.6 \cdot C_{H_2O_t}$ (Behrens and Stuke, 2003).
Concentrations of H₂O molecules (C_{H_2O}) and OH groups (C_{OH}) are calculated from TT baseline-corrected values of A_{5200} and A_{4500} using the calibration B. For error bars of C_{OH} and C_{H_2O} see Fig. 7A and B.
Estimated errors are ±0.05 wt.% for $C_{H_2O_t}$, ±2 μm for thickness, 1% for density, ±0.003 for A_{4500} and A_{5200} (FC), ±0.002 for A_{4500} and A_{5200} (TT), ±2 cm⁻¹ for $A_{4500}*$ and $A_{5200}*$ (FC). [a]Sample were measured in the main chamber of the FTIR spectrometer using an InSb detector. [b]Glass was synthesized for this study, other glasses are described in Behrens and Stuke (2003).

the OH band shifts slightly to lower wave numbers (from 4505 ± 4 cm⁻¹ at 1 wt.% H₂Oₜ to 4490 ± 4 cm⁻¹ at 6 wt.% H₂Oₜ) but the width of the band does not change noticeably. The position of the maximum near 5200 cm⁻¹ does not change upon hydration (exact position at 5220 ± 4 cm⁻¹) but the shoulder at 5000 cm⁻¹ decreases in intensity. The same trends are observed for SLS glass.

Although there are variations in position and shape of the NIR bands, peak areas and peak heights are simply linearly correlated (Fig. 3A and B). For the 4500 cm⁻¹ band both quantities are proportional. For the 5200 cm⁻¹ band the regression line does not pass through the origin, this is particularly noticeable for

the FG glass. The positive peak area at zero peak height implies an additional contribution to the peak area that is not related to dissolved water. However, this effect could be an artefact of the baseline correction due to incomplete separation of the combination bands. It is noteworthy, that in general the determination of peak height has a much better reproducibility than determination of peak area, as illustrated in Fig. 3A and B.

3.2. Determination of species concentration

Assuming that all hydrous species are represented by the two bands at 4500 and 5200 cm⁻¹, the
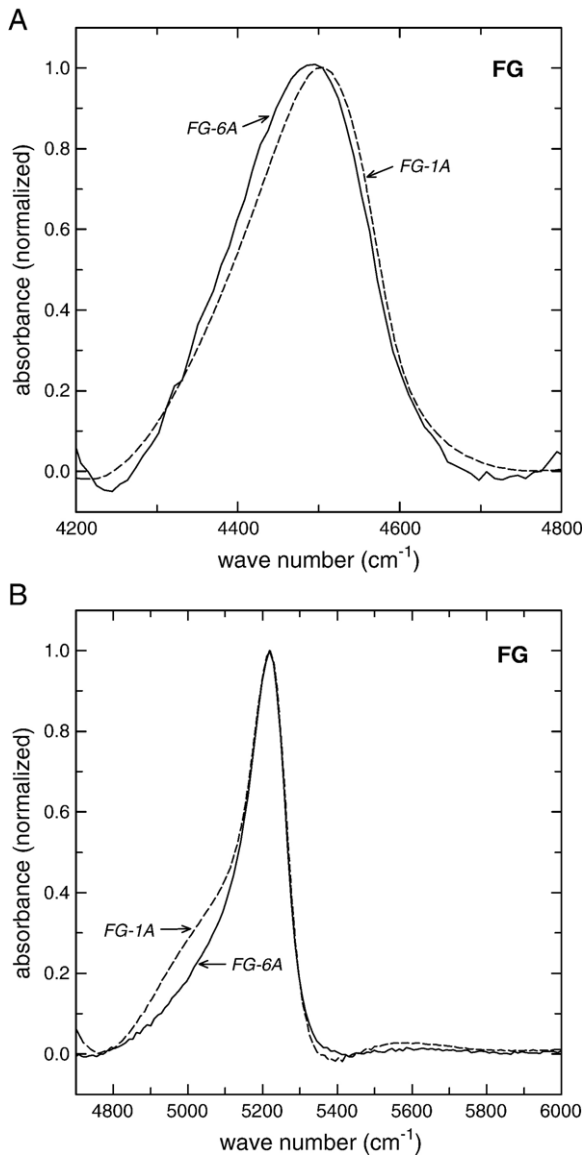
Fig. 2. Baseline-corrected spectra of float glass with water content 1.18 and 5.67 wt.%. Note the shift of the OH band (A) and the relative decrease in intensity of the shoulder at 5200 cm^{-1} (B).

concentrations of the species can be determined from the peak intensities using the Lambert–Beer law:

$$C_{OH} = \frac{1802 \cdot A_{4500}}{d \cdot \rho \cdot \varepsilon_{4500}} \qquad (3)$$

$$C_{H_2O} = \frac{1802 \cdot A_{5200}}{d \cdot \rho \cdot \varepsilon_{5200}} \qquad (4)$$

where A denotes the absorbance (peak height), d the thickness in cm, ρ the density in g/l, and ε the linear

molar absorption coefficient (sometimes referred to as the molar extinction coefficient or the molar absorptivity) in L mol^{-1} cm^{-1}. C_{OH} and C_{H_2O} are the concentrations of water dissolved as OH groups and molecular H_2O, respectively, in wt.%. Density was calculated according to Behrens and Stuke (2003). The total water concentration, $C_{H_2O_t}$, is given by the sum of the concentrations of the two species.

Assuming that the absorption coefficients are independent of the total water content, one expects a linear relationship between the normalized absorbances A_{5200}^{norm} and A_{4500}^{norm} (expressions in square bracket in Eq. (5))

$$\left[\frac{1802 \cdot A_{H_2O}}{d \cdot \rho \cdot C_{H_2O_t}} \right] = \varepsilon_{H_2O} - \frac{\varepsilon_{H_2O}}{\varepsilon_{OH}} \left[\frac{1802 \cdot A_{OH}}{d \cdot \rho \cdot C_{H_2O_t}} \right]. \qquad (5)$$

Fig. 4 shows plots of normalized absorbances for FG and SLS glasses using tangent baseline corrections. Plots for the FC baseline are similar with slightly higher values of normalized absorbances (see Fig. 1B). A major problem in fitting the FC baseline was to select points on the absorbance curve, which are not influenced by the bands of interest. As a consequence, the reproducibility of absorbance measurement was significantly lower for the FC baseline than for the TT baseline. For example, a triplicated evaluation of the same spectrum (FG0-25D) shows a variation in peak height of the 4500 cm^{-1} band between 0.065 and 0.071 for FC baseline and between 0.063 and 0.065 for TT baseline. Hence, we have chosen the latter one for the standard procedure.

For both compositions the normalized absorbances are approximately linearly correlated (dashed lines in Fig. 4). Provided that the molar absorption coefficients are constant, their values can be read as the intersections of the regression line with the axis (further on this approach will be denoted as calibration A). The determined values of ε_{4500} agree within error for FG and SLS glass whereas ε_{5200} is slightly higher for FG than for SLS glass (Table 4).

3.3. ^{1}H NMR spectroscopy

Low temperature (140 K) static ^{1}H NMR spectra of hydrous soda lime silica glass and float glass are shown in Fig. 5A and B, respectively. The spectra consist of two overlapping components. The broad central line is attributed to OH groups and superimposed on this signal is the Pake doublet which is due to strong dipolar coupling of protons in immobilized H_2O molecules (Bartholomew and Schreurs, 1980). At
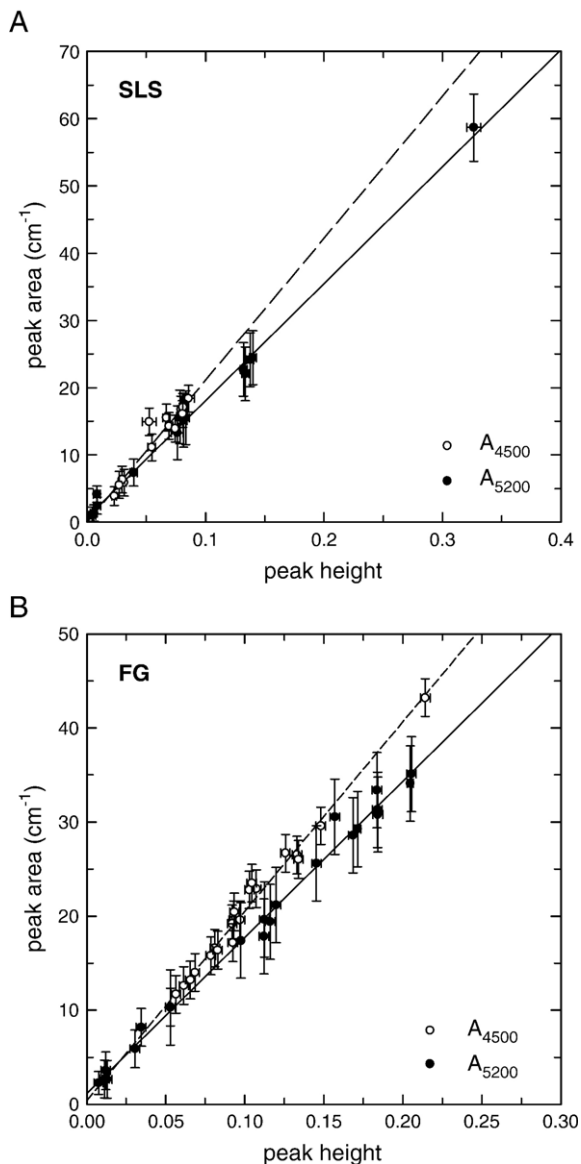
A

B

Fig. 3. Peak area versus peak height for the combination bands using a flexi curve for baseline correction of (A) SLS and (B) FG glass. Dashed lines are linear regression for the 4500 cm^{-1} band and solid lines represent linear regression for the 5200 cm^{-1} band.

molecules in our glasses. Only in the case of pure silica and silica-rich aluminosilicate glasses lower temperatures are needed to immobilize H_2O molecules (Schmidt et al., 1999).

NMR spectra are decomposed into a Pake-doublet and a central signal as described in Schmidt et al. (2001). The ratio of areas below the signals (central line/Pake doublet) corresponds to the ratio of protons in OH groups to those in H_2O molecules. Three SLS glasses and one FG glass were investigated by low temperature static ^{1}H NMR spectroscopy. Results are presented in Table 3.

4. Discussion

4.1. Comparison of water speciation by NMR and NIR

OH concentrations based on low temperature static ^{1}H NMR spectroscopy deviate significantly from OH concentrations calculated from NIR spectra using the absorption coefficients determined by the internally consistent calibration A. For SLS glasses C_{OH} derived from NMR measurements is systematically higher than values based on NIR spectroscopy (e.g., 2.19 wt.% based on NMR and 1.56 wt.% based on NIR for SLS-7NMR, see Table 3). An opposing trend is observed for FG glass with lower OH contents predicted by NMR spectroscopy (1.52 wt.% compared to 2.04 wt.%
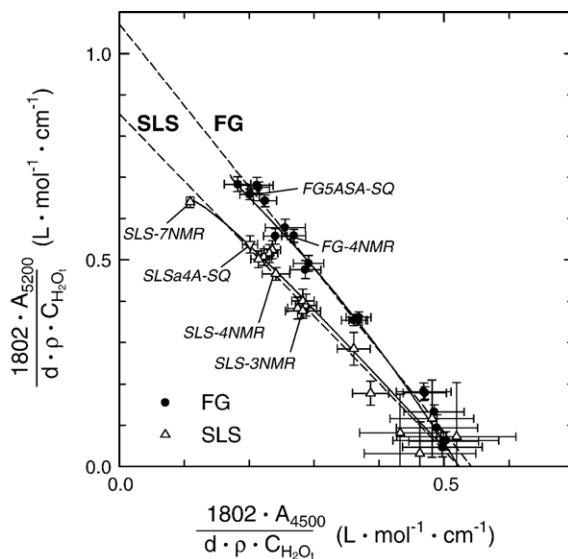

Fig. 4. Plot of normalized absorbances for the 4500 and the 5200 cm^{-1} band using TT baseline correction for (a) SLS glass and (b) FG glass. Dashed line represents the fits assuming constant absorption coefficients (calibration A). Solid line shows the trend for absorption coefficients varying linearly with water content (calibration B).
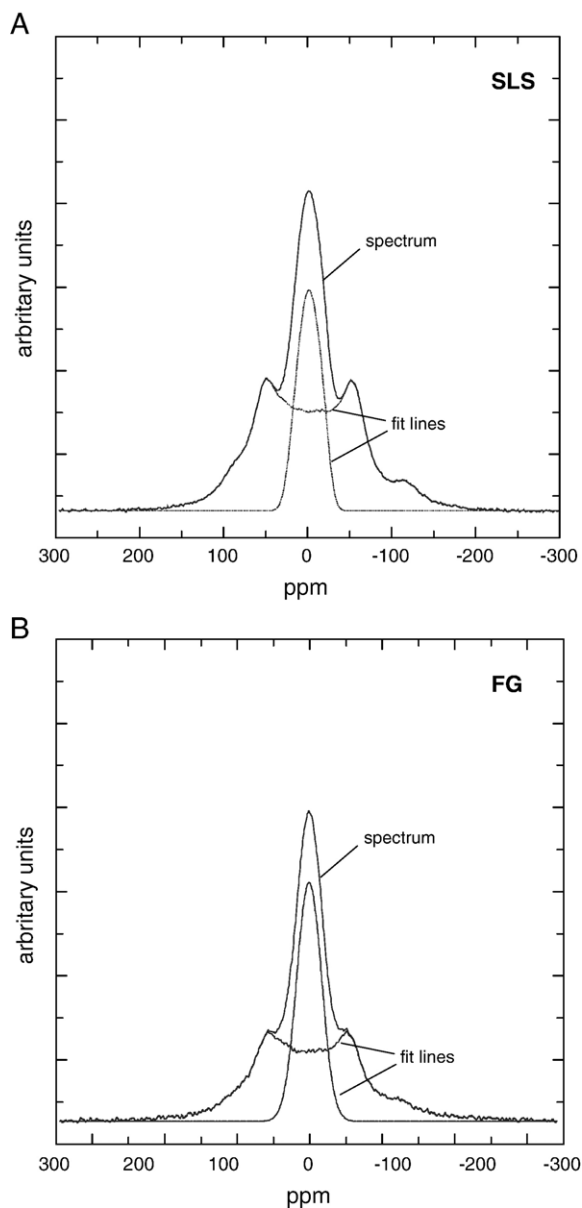
higher temperatures the intensity of the central peak increases relative to that of the Pake doublet due to the activation of rotation of H_2O molecules, which now contribute to the central part of the signal (Bartholomew and Schreurs, 1980; Zavel'sky et al., 1998; Schmidt et al., 2001). We have not carried out measurements at other temperatures, but findings on alkali silicate glass and zinc alkali silicate glass (Bartholomew and Schreurs, 1980) as well as aluminosilicate glasses (Schmidt et al., 2001) suggest that a temperature of 140 K is sufficient to freeze in motions of H_2O

A

B

Fig. 5. Static ^{1}H NMR spectrum of hydrous glasses recorded at 140 K. (A) Soda lime silica glass SLS 4NMR containing 7.42 wt.% H_2O_t. (B) Float glass FG 4 NMR containing 3.99 wt.% H_2O_t. The spectra are fitted with a single central line assigned to OH groups and a Pake doublet assigned to H_2O molecules.

derived from NIR spectroscopy for FG-4NMR). These discrepancies imply that the assumption of constant absorption coefficients for the NIR bands may be incorrect for float glass and soda lime silica glass.

Zarubin (1999) argued that the NIR combination bands represent mainly hydrous species that are weakly H-bonded. Thus the combination band at 5200 cm^{-1} results from simultaneous excitation of the H_2O bending vibration near 1650 cm^{-1} and OH stretching vibrations near 3550 cm^{-1}. The intensity ratio for mid-infrared absorption bands at 3550 cm^{-1} (caused by weakly H-bonded hydrous species) and 2850 cm^{-1} (caused by strongly H-bonded hydrous species) grows continuously with increasing water content (Behrens and Stuke, 2003). Hence, intuitively one might expect that the NIR absorption coefficients increase with water content. This trend was indeed observed by Peuker et al. (2003) for various silicate and aluminosilicate glasses containing up to 0.12 wt.% H_2O_t. However, the range of water content in that study was small and it remained an open question whether the trend can be extrapolated towards high water content.

4.2. Variation of the NIR absorption coefficients with water content

In an improved calibration of the NIR absorption coefficients (hereafter denoted as calibration B) we have considered a possible variation of the NIR absorption coefficients with water content. Quench rate in the range of 0.2–50 K/s was found to have no measurable effect on NIR absorption coefficients for haplogranitic glasses (Behrens and Nowak, 2003). Most of our FG and SLS glasses were quenched at a rate of ~2 K/s through the range of glass transition. Two slow quench samples (~0.1 K/s) fall on trend lines in Fig. 4 implying that the absorption coefficients are applicable also for slowly cooled glasses, but more data with different water contents and quench rates are required to verify this hypothesis. In calibration B we assume that cooling rate has no effect on absorption coefficients and variations are related only to total water content.

In order to evaluate the dependence of absorption coefficients on water content we have two sources of information. First, an independent calibration of the absorption coefficients for the 4500 and the 5200 cm^{-1} band can be performed for some hydrous glasses using the NMR data. Second, in glasses with low water content the concentration of OH groups is much larger than that of H_2O molecules so that at least the value of ε_{4500} can be predicted very well. For example, the A_{5200}/A_{4500} ratio is only 1/15 for sample SLS-NRA2 containing 0.51 wt.% H_2O_t (Table 2). As an approximation OH concentrations in water-poor glasses were estimated using the total water content minus the molecular H_2O content determined by calibration A. When doing so, the error of OH concentration is still dominated by the error of bulk water determination for glasses containing less than 1 wt.% H_2O_t.

Table 3
Comparison of water speciation determined by static ^{1}H NMR spectroscopy and by NIR spectroscopy (TT baseline) using calibration A

Sample	$C_{H_2O_t}$ (wt.%)	$C_{H_2O_t}$ (mol/L)	$C_{OH}/C_{H_2O_t}$ NMR	C_{OH} NMR (wt.%)	Density (g/L)	Thickness (cm)	A_{4500}	A_{5200}	C_{OH} NIR (wt.%)	ε_{4500} (L mol^{-1} cm^{-1})	ε_{5200} (L mol^{-1} cm^{-1})
SLS-3NMR	2.86±0.05	3.91	0.575±0.030	1.64	2464	0.0483	0.053	0.071	1.54	0.50±0.04	0.89±0.06
						0.0494	0.055	0.073	1.57		
SLS-4NMR	3.59±0.06	4.89	0.510±0.040	1.83	2453	0.0488	0.058	0.107	1.67	0.47±0.04	0.95±0.08
						0.0495	0.058	0.117	1.66		
SLS-7NMR	7.42±0.05	9.87	0.295±0.030	2.19	2397	0.0513	0.055	0.324	1.56	0.37±0.04	0.91±0.09
FG-4NMR	4.07±0.07; 3.91±0.07	5.48	0.382±0.040	1.52	2469	0.0514	0.076	0.157	2.04	0.71±0.08	0.90±0.10

Total water content was measured by KFT. If two sets of data are given, these sets correspond to measurements on samples cut from both ends of the synthesized glass. Absorption coefficients were calculated using the average of NIR measurements from both ends.

Absorption coefficients for three SLS glasses containing 0.5–0.8 wt.% H_2O_t are similar to the value of 0.53 L mol^{-1} cm^{-1} reported by Peuker et al. (2003) for water enriched soda lime silica glass (0.12 wt.% H_2O_t) implying that the strong increase of ε_{4500} with $C_{H_2O_t}$ observed at low water content (Peuker et al., 2003) does not proceed to higher water contents (Fig. 6A). However, it has to be emphasized that the tangent baseline applied in our study and in that of Peuker et al. (2003) increasingly underestimates the peak height at 4500 cm^{-1} with decreasing water content because it does not account for the curvature of the tail of the OH stretching vibration band. Hence, the strong increase of the 4500 cm^{-1} absorption coefficient observed by Peuker et al. (2003) at low water content may be due to the choice of the baseline.

For SLS glass ε_{4500} decreases linearly with $C_{H_2O_t}$ from 0.54 L mol^{-1} cm^{-1} at 0.5 wt.% H_2O_t to 0.38 L mol^{-1} cm^{-1} at 7.5 wt.% H_2O_t. (Fig. 6A). The dependence of ε_{4500} on water content is not well constrained for FG glass due to a lack of samples measured by NMR spectroscopy. For simplicity we assume also a linear variation (Fig. 6B). The opposing trends for FG and SLS imply that chemical composition has not only strong influence on the magnitude of the NIR absorption coefficients but also on their dependence on $C_{H_2O_t}$.

Assuming a linear variation of ε_{4500} with $C_{H_2O_t}$ (Table 3) we have calculated the OH concentrations for all glasses based on the NIR spectra. The difference between total water and OH content is interpreted as the concentration of H_2O molecules. Next, the absorption coefficient for the 5200 cm^{-1} band is calculated for each glass. Only glasses with water contents above 2 wt.% were considered because otherwise the relative error of C_{H_2O} is too large to yield reliable absorption coefficients. No significant variation of ε_{5200} with $C_{H_2O_t}$ was found for both glass compositions (Fig. 6A and B). Average values of ε_{5200} are similar for FG and SLS glass (0.89 and 0.95 L mol^{-1} cm^{-1}, respectively). However, it has to be emphasized that using a constant value of ε_{5200} may introduce an unknown systematic error in molecular H_2O concentration at $C_{H_2O_t}$ below 2 wt.%.

Using calibration B we have calculated the expected trends in the plot of normalized absorbances (solid lines in Fig. 4). Water speciation data shown in Fig. 7A and B (solid line) were used in this calculation and, hence, the trend line corresponds to a cooling rate of ~2 K/s. Both calibrations A and B reproduce the trend of the data in Fig. 4 very well. Our conclusion from this finding is that a good fit of the spectroscopic data in such a plot is not sufficient to support the assumption of constant
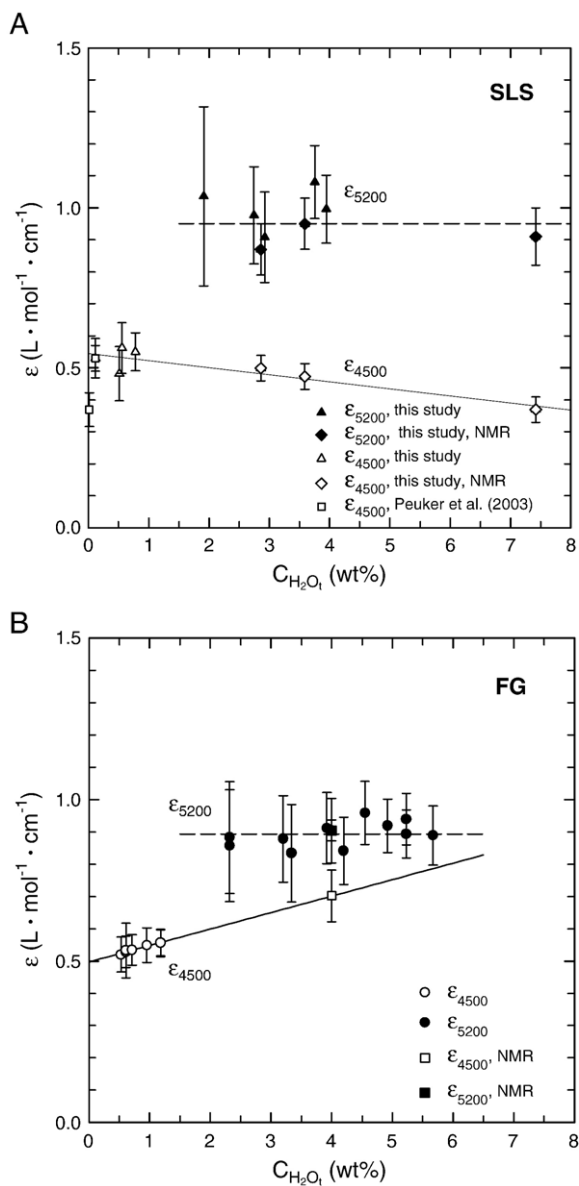
Fig. 6. Variation of absorption coefficients with water content derived by calibration *B* for SLS glass (A) and FG glass (B).

absorption coefficients (calibration *A*). Therefore, an external calibration is needed for verification.

4.3. Variation of molar absorption coefficients with glass composition

Dixon et al. (1995) noticed simple linear relationships between the molar absorption coefficients for the near-infrared combination bands at 4500 and 5200 cm^{-1} and the tetrahedral cation fraction $\tau (=[Al^{3+}+Si^{4+}]/$ sum of cations). Later calibrations (Jakobsson, 1997; Yama-

shita et al., 1997; Ohlhorst et al., 2001; Mandeville et al., 2002) confirm the trend of increasing absorption coefficients with increasing cation fraction of $Al^{3+}+Si^{4+}$ which can be used for the prediction of absorption coefficients. Using 22 calibrations for the range $0.621 < \tau < 0.860$, Mandeville et al. (2002) calculated linear regressions for both absorption coefficients ($\varepsilon_{4500} = -2.026 + 4.054 \cdot \tau$ and $\varepsilon_{5200} = -2.463 + 4.899 \cdot \tau$). The predictions of Mandeville et al. (2002) for our compositions ($\tau = 0.64$) are $\varepsilon_{4500} = 0.57$ L mol^{-1} cm^{-1} and $\varepsilon_{5200} = 0.67$ L mol^{-1} cm^{-1}. The experimental ε_{4500} values for water-poor float glass and soda lime silica glass are in good agreement with the predictions for both the internal calibration *A* of NIR spectra using bulk composition only and the calibration *B* supported by NMR data (Table 4). On the other hand, experimental ε_{5200} values are significantly higher than those predicted (by 33% for FG and by 46% for SLS when using calibration *B*).

The discrepancies between predicted and experimental ε_{5200} values for FG and SLS glass, as well as the large scatter of data in the calibration of the regressions of Mandeville et al. (2002) imply that a single parameter such as the cation fraction of $Al^{3+}+Si^{4+}$ is not sufficient to reproduce all the compositional variation of the absorption coefficients for silicate melts. As shown in previous studies the molar absorption coefficients of OH and H_2O combination bands depend on several composition parameters such as SiO_2 content (Ohlhorst et al., 2001), the ratio of Na/K (Behrens et al., 1996), the concentration of alkaline earth elements or the excess of alkali to aluminium (Stolper, 1982a,b; Silver et al., 1990; Behrens et al., 1996). For instance, when exchanging alkalis in glasses with alkali feldspar composition ε_{5200} increases from 1.12 (for Li) to 1.49 (for Na) to 1.65 (for K) (Behrens et al., 1996). In conclusion, simple relationships can be used as a rough estimate for the absorption coefficients but the uncertainty is too high for a precise determination of species concentrations.

4.4. Water speciation in float glass and soda lime silica glass

To check the influence of the IR calibration method on water speciation, the concentrations of OH groups and H_2O molecules in FG and SLS glasses were calculated using concentration dependent ε values supported by NMR data (calibration *B*; Fig. 7A and B) as well as using ε values calibrated against bulk water contents only (calibration *A*; Fig. 7C and D). The overall evolution of species concentrations with total water content is similar for both IR calibrations in that the OH
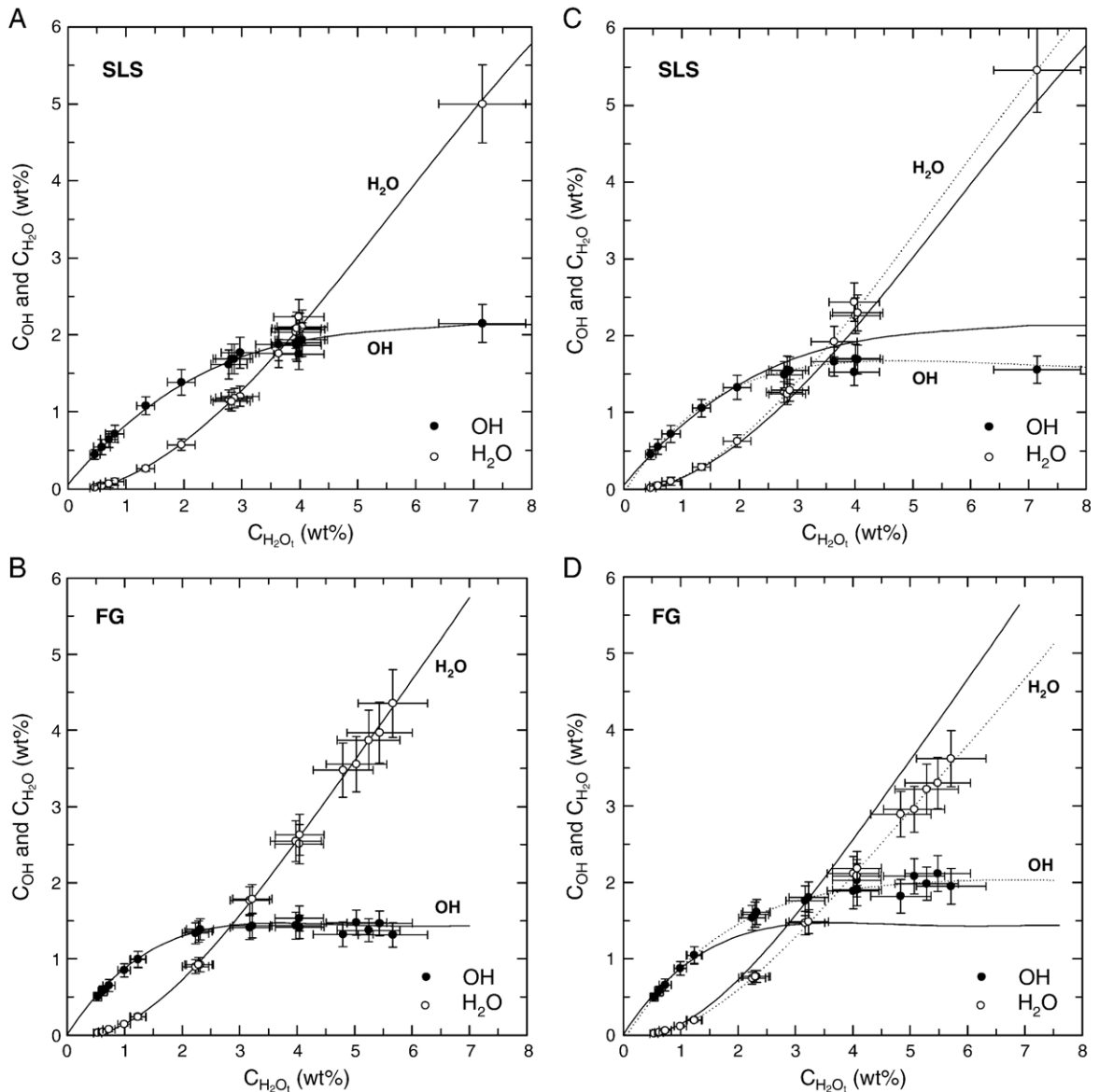
Fig. 7. Concentrations of OH groups and H_2O molecules as a function of total water content for SLS (A) and FG (B) glass based on TT baseline/absorbance measurement and calibration B.. For comparison results from calibration A (constant absorption coefficients) are shown for SLS in (C) and FG in (D). Solid lines refer to water speciation based on calibration B. Dashed lines indicate the trends for calibration A.

content increases strongly with water content at low $C_{H_2O_t}$ and reaches an apparent saturation value at high $C_{H_2O_t}$. The apparent saturation value is higher for calibration A in the case of FG glass (2.0 wt.% compared to 1.4 wt.%) but lower in the case of SLS glass (1.6 wt.% compared to 2.2 wt.%). Hence, the internally consistent calibration A overestimates the OH content in FG glass by up to 57% but it underestimates the OH content in SLS glass by up to 27%. The different trends for both compositions are a direct consequence of the relative abundance of hydrous species in the glasses analyzed by

NMR measurements. For the preferred IR calibration B supported by the NMR results the transition from OH dominated to H_2O dominated water speciation is at lower water content for FG (near 3 wt.%) than for SLS (near 4 wt.%). It is unlikely that the small difference in silica content and in glass polymerization (expressed as the ratio of non-bridging oxygen to tetrahedral cations, NBO/T, see Table 1) is the source for the different trends of ε_{4500} and C_{OH}. A major difference between FG and SLS glasses is the concentration of alkaline-earth elements and the Ca/Mg ratio. Support for the

hypothesis that alkaline-earth elements have different effects on water speciation and NIR absorption coefficients than alkali elements is given by a study on glasses along the join $NaAlSi_3O_8$–$Ca_{0.5}AlSi_3O_8$ (Ohlhorst et al., 2000). It was found that substitution of alkaline-earth element for alkali elements stabilize H_2O molecules in the glasses, increases ε_{4500} but decreases ε_{5200}.

Slow quench rates (5 K/min compared to 100 K/min) decrease slightly the concentration of OH groups in the glasses, consistent with observations in previous studies on aluminosilicate glasses (Silver et al., 1990; Behrens and Nowak, 2003). After reheating under pressure and subsequent slow quench, C_{OH} in glass SLSa-A4 was reduced from 1.95 to 1.75 wt.% with a corresponding increase in CH_2O from 2.10 to 2.23 wt.%. In sample FG5AS-A processed in the same experiment, C_{OH} decreases from 1.47 to 1.37 wt.%, but CH_2O decreases also (from 3.97 to 3.87 wt.%), probably due to water loss during the slow quench experiment. The variation of the relative abundance of hydrous species with quench rate reflects the temperature dependence of water speciation in the melt. With faster quench a higher fictive temperature (apparent equilibrium temperature of the melt) is frozen in (Dingwell and Webb, 1990) and the relative abundance of OH groups increases with temperature (Sowerby and Keppler, 1999; Nowak and Behrens, 2001).

4.5. Absorption coefficient for the 1630 cm^{-1} band

The new calibrations yield molecular H_2O concentrations for FG and SLS glasses which are much higher than previous estimates based on the peak height of the
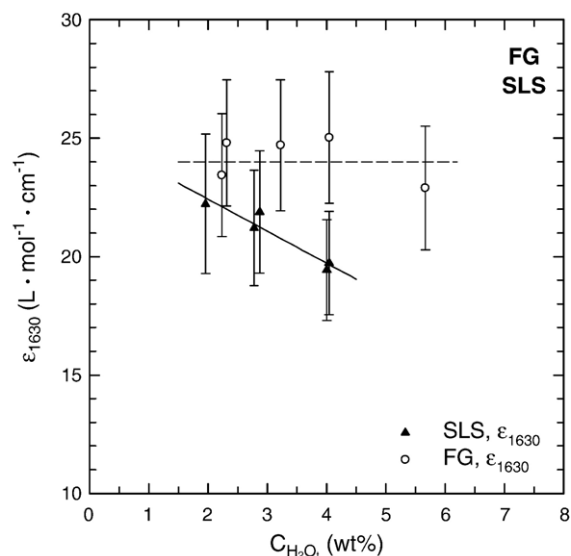

Fig. 8. Absorption coefficient for 1630 cm^{-1} band as function of total water content based on molecular H_2O contents of Fig. 7. Absorbances for 1630 cm^{-1} were taken from Behrens and Stuke (2003). The dashed line marks the average value for FG glass. The solid line is a linear regression to data for SLS glass.

1630 cm^{-1} band (Behrens and Stuke, 2003). This implies that the absorption coefficient for the 1630 cm^{-1} band (ε_{1630}) of 49 L mol^{-1} cm^{-1} which has been used in the preliminary calculation is significantly too high. Based on the new water speciation data (NIR, calibration B) we have calculated ε_{1630} for each sample for which both near-infrared and mid-infrared spectra were recorded. Between 1.5 and 6 wt.% total water content ε_{1630} shows no significant variation with $C_{H_2O_t}$ for FG glass (Fig. 8). Data for SLS glass indicate a slight decrease of ε_{1630} with total water, but within error the data are also consistent with a constant absorption coefficient. Average values are 24.2 ± 1.0 L mol^{-1} cm^{-1} for FG and 20.9 ± 1.3 L mol^{-1} cm^{-1} for SLS. These value are in good agreement with the prediction of 27 L mol^{-1} cm^{-1} based on the relationship between cation fraction and ε_{1630} proposed by Mandeville et al. (2002) as well as with experimental determinations for other depolymerized glasses such as a basalt (25 L mol^{-1} cm^{-1}; Dixon et al., 1995) or a complex Zn-bearing silicate glass (28 L mol^{-1} cm^{-1}; Bartholomew et al., 1980). It is noteworthy that the value of 26 L mol^{-1} cm^{-1} estimated by Scholze et al. (1975) from the uptake of water during corrosion of soda-lime-silica glasses also is close to our determination.

5. Conclusions

Discrepancies were observed for hydrous species concentrations (OH groups and H_2O molecules) in float

Table 4
Absorption coefficients (L mol^{-1} cm^{-1})

	SLS		FG	
	ε	σ_ε	ε	σ_ε
ε_{4500}, TT, calibration B	$(0.54 \pm 0.02) -$ $(0.022 \pm 0.005) \cdot$ $C_{H_2O_t}$	0.030	$(0.497 \pm 0.004) +$ $(0.051 \pm 0.002) \cdot$ $C_{H_2O_t}$	0.006
ε_{5200}, TT, calibration B	0.95	0.06	0.89	0.06
ε_{4500}, TT, calibration A	0.52	0.03	0.53	0.01
ε_{5200}, TT, calibration A	0.87	0.04	1.07	0.02
ε_{1630}	20.9	1.3	24.2	1.0

Calibration B supported by NMR data is recommended for determination of hydrous species. Calibration A is suitable to determine the total water content but does not reproduce accurately species concentrations. ε_{1630} is the mean value derived from spectroscopic data of Behrens and Stuke (2003) and molecular H_2O concentrations reported in Table 3. σ_ε = standard error of ε.

glass and soda lime silica glass between determinations by low temperature static ^{1}H NMR spectroscopy and by NIR spectroscopy, when using constant absorption coefficients for evaluation of the peak heights of the NIR combination bands at 4500 and 5200 cm^{-1}. The discrepancies can be explained by variation of the absorption coefficients with the total water content. It appears that in particular the absorption coefficient of the OH combination band at 4500 cm^{-1} varies with water content for these glass compositions. For float glass we found an increase of ε_{4500} by 35% relative when the water content increases from 0.5 to 4.0 wt.%. This trend is consistent with findings of Peuker et al. (2003) for simple silicate glasses with low water contents (<0.2 wt.%). On the other hand, soda lime glass shows a systematic linear decrease of ε_{4500} by 27% between 0.5 and 7.5 wt.% H$_2$O$_t$, opposite to the trend expected from studies at low water content. The absorption coefficient for the molecular H$_2$O combination band at 5200 cm^{-1} appears to be less dependent on water content. Variation of ε_{5200} is within 10% for FG and SLS glass and correlation of ε_{5200} with total water content is not evident. However, because only glasses containing more than 2.0 wt.% H$_2$O$_t$ were used in the calibration of ε_{5200}, we cannot exclude a dependence of ε_{5200} on $C_{H_2O_t}$ at low water content.

Our findings are consistent with the suggestion of Zarubin (1999) that the NIR bands represent only the weakest hydrogen bonded water species in the glasses. Constant absorption coefficients are only suitable when the relative abundance of weakly and strongly H-bonded species is not changing with composition/water content. This seems not to be the case for float glass and soda lime silica glass. Variations of the NIR absorption coefficients with bulk water content can also be expected for other silicate glasses displaying intensive OH stretching bands of strongly H-bonded species (typically a set of bands with maxima near 2850, 2350 and 1750 cm^{-1}, denoted as ABC pattern (Zarubin, 1999). Findings of Peuker et al. (2003) suggest that an increasing relative abundance of weakly H-bonded species with increasing total water content is typical for such silicate glasses. On the other hand, depolymerized aluminosilicate glasses such as andesite or basalt show relatively simple OH-stretching bands dominated by weakly H-bonded species (Stolper, 1982a,b; Mandeville et al., 2002). The NIR absorption coefficients for andesite and basalt calibrated on the basis of total water content are smaller by a factor of 2 to 3 compared to rhyolite (Ohlhorst et al., 2001; Mandeville et al., 2002; and references therein). The low absorption coefficients may reflect that only a minor part of hydrous species contributes to the NIR combination bands and it has to be tested by independent quantification of hydrous species whether the assumption that ε values are independent on water content is justified or not.

At high total water contents the OH concentration in float glass and soda lime glass reaches an apparent saturation level of 1.4 and 2.2 wt.%, respectively. These values are within the range of maximum OH contents found for various aluminosilicate glasses quenched at similar rate from melt to glass (1.5–2.2 wt.% water dissolved as OH), although composition and glass transition temperatures vary widely (Silver et al., 1990; Behrens et al., 1996; Withers and Behrens, 1999; Ohlhorst et al., 2001; Schmidt et al., 2001; Mandeville et al., 2002; Behrens and Nowak, 2003). Higher OH concentrations can be adjusted in thermodynamic equilibrium in melts at high temperature (e.g., Nowak and Behrens, 2001) but cannot be frozen in glasses even when using rapid quench.

References

Baker, D.R., 1991. Interdiffusion of hydrous dacitic and rhyolitic melts and the efficacy of rhyolite contamination by dacitic enclaves. Contrib. Mineral. Petrol. 106, 462–473.

Bartholomew, R.F., Schreurs, J.W.H., 1980. Wide-line NMR study of protons in hydrosilicate glasses of different water content. J. Non-Cryst. Solids 38&39, 679–684.

Bartholomew, R.F., Butler, B.L., Hoover, H.L., Wu, C.K., 1980. Infrared spectra of water-containing glass. J. Am. Ceram. Soc. 63, 481–485.

Behrens, H., Nowak, M., 2003. Quantification of H$_2$O speciation in silicate glasses and melts by IR spectroscopy—in situ versus quench techniques. Phase Transit. 76, 45–61.

Behrens, H., Stuke, A., 2003. Quantification of H$_2$O contents in silicate glasses using IR spectroscopy—a calibration based on hydrous glasses analyzed by Karl–Fischer titration. Glass Sci. Technol. 76, 1–14.

Behrens, H., Romano, C., Nowak, M., Holtz, F., Dingwell, D.B., 1996. Near-infrared spectroscopic determination of water species in glasses of the system MAlSi$_3$O$_8$ (M=Li, Na, K): an interlaboratory study. Chem. Geol. 128, 41–64.

Behrens, H., Kappes, R., Heitjans, P., 2002. Proton conduction in glass —an impedance study on hydrous BaSi$_2$O$_5$ glass. J. Non-Cryst. Solids 306, 271–281.

Dingwell, D.B., Webb, S.L., 1990. Relaxation in silicate melts. Eur. J. Mineral. 2, 427–449.

Dixon, J.E., Stolper, E.M., Holloway, J.R., 1995. An experimental study of water and carbon dioxide in mid-ocean ridge basaltic liquids: Part I. Calibration and solubility models. J. Petrol. 36, 1607–1631.

Eckert, H., Yesinowski, J.P., Silver, L.A., Stolper, E.M., 1988. Water in silicate glasses: quantization and structural studies by ^{1}H solid echo and MAS-NMR methods. J. Phys. Chem. 92, 2055–2064.

Giordano, D., Dingwell, D.B., 2003. Viscosity of hydrous Etna basalt: implications for Plinian-style basaltic eruptions. Bull. Volcanol. 65, 8–14.

Giordano, D., Romano, C., Dingwell, D.B., Poe, B., Behrens, H., 2004. The combined effects of water and fluorine on the viscosity of silicic magmas. Geochim. Cosmochim. Acta 68, 5159–5168.

Hess, K.-U., Dingwell, D.B., 1996. Viscosities of hydrous leucogranitic melts: a non-Arrhenian model. Am. Mineral. 81, 1297–1300.

Jakobsson, S., 1997. Solubility of water and carbon dioxide in an icelandite at 1400 °C and 10 kilobars. Contrib. Mineral. Petrol. 127, 129–135.

Koepke, J., Behrens, H., 2001. Trace element diffusion in andesitic melts—an application of synchrotron X-ray fluorescence analysis. Geochim. Cosmochim. Acta 65, 1481–1498.

Kohn, S.C., Dupree, R., Smith, M.E., 1989. Proton environments and hydrogen-bonding in hydrous silicate glasses from proton NMR. Nature 337, 539–541.

Mandeville, C.W., Webster, J.D., Rutherford, M.J., Taylor, B.E., Timbal, A., Faure, K., 2002. Determination of molar absorptivities for infrared absorption bands of H_2O in andesitic glasses. Am. Mineral. 87, 813–821.

Nowak, M., Behrens, H., 2001. Water in magmas: getting grip on a slippery problem. Earth Planet. Sci. Lett. 184, 515–522.

Ohlhorst, S., Behrens, H., Holtz, F., Schmidt, B.C., 2000. Water speciation in aluminosilicate glasses and melts. In: Rammlmair, D., Mederer, J., Oberthür, Th., Heimann, R.B., Pentinghaus, H. (Eds.), Applied Mineralogy in Research, Economy, Technology and Culture. Proc. 6th Int. Conf. Appl. Mineral., vol. 1. Balkema, Rotterdam, pp. 193–196.

Ohlhorst, S., Behrens, H., Holtz, F., 2001. Compositional dependence of molar absorptivities of near-infrared OH– and H_2O bands in rhyolitic to basaltic glasses. Chem. Geol. 174, 5–20.

Persikov, E.S., Zharikov, V.A., Bukhtiyarov, P.G., Pol'skoy, S.F., 1990. The effect of volatiles on the properties of magmatic melts. Eur. J. Mineral. 2, 621–642.

Peuker, C., Reinholz, U., Jäger, C., Pauli, J., Geißler, H., 2003. Extinction coefficients of the OH bands in the IR spectra of basic and water-enriched silicate and aluminosilicate glasses. Glass Sci. Technol. 76, 276–284.

Richet, P., Lejeune, A.M., Holtz, F., Roux, J., 1996. Water and the viscosity of andesite melts. Chem. Geol. 128, 185–197.

Richet, P., Whittington, A., Holtz, F., Behrens, H., Ohlhorst, S., Wilke, M., 2000. Water and the density of silicate glasses. Contrib. Mineral. Petrol. 138, 337–347.

Robert, E., Whittington, A., Fayon, F., Pichavant, M., Massiot, D., 2001. Structural characterization of water-bearing silicate and aluminosilicate glasses by high-resolution solid-state NMR. Chem. Geol. 174, 291–305.

Romano, C., Hess, K.-U., Mincione, V., Poe, B., Dingwell, D.B., 2001. The viscosities of hydrous XAlSi$_3$O$_8$ (X=Li, Na, K, Ca$_{0.5}$, Mg$_{0.5}$) melts. Chem. Geol. 174, 115–132.

Schmidt, B.C., Riemer, T., Kohn, S.C., Behrens, H., Dupree, R., 1999. Different water solubility mechanisms in hydrous glasses along the Qz–Ab join. Evidence from NMR spectroscopy. Geochim. Cosmochim. Acta 64, 513–526.

Schmidt, B.C., Behrens, H., Riemer, T., Kappes, R., Dupree, R., 2001. Quantitative determination of water speciation in aluminosilicate glasses: a comparative NMR and IR spectroscopic study. Chem. Geol. 174, 195–208.

Scholze, H., 1960. Zur Frage der Unterscheidung zwischen H_2O-Molekülen und OH-Gruppen in Gläsern und Mineralen. Naturwissenschaften 47, 226 (in German).

Scholze, H., Holmreich, D., Barkardijev, I., 1975. Untersuchungen über das Verhalten von Kalk–Natron–Gläsern in verdünnten Säuren. Glastech. Ber. 48, 237–347 (in German).

Schulze, F., Behrens, H., Holtz, F., Roux, J., Johannes, W., 1996. The influence of H_2O on the viscosity of a haplogranitic melt. Am. Mineral. 81, 1155–1165.

Silver, L.A., Ihinger, P.D., Stolper, E.M., 1990. The influence of bulk composition on the speciation of water in silicate glasses. Contrib. Mineral. Petrol. 104, 142–162.

Sowerby, J.R., Keppler, H., 1999. Water speciation in rhyolitic melt determined by in situ infrared spectroscopy. Am. Mineral. 84, 1843–1849 (erratum in 85, 880).

Stolper, E.M., 1982a. Water in silicate glasses: an infrared spectroscopic study. Contrib. Mineral. Petrol. 81, 1–17.

Stolper, E., 1982b. The speciation of water in silicate melts. Geochim. Cosmochim. Acta 46, 2609–2620.

Watson, E.B., 1994. Diffusion in volatile-bearing magmas. Rev. Mineral. 30, 371–411.

Whittington, A., Richet, P., Behrens, H., Holtz, F., Scaillet, B., 2004. Experimental temperature–$X(H_2O)$–viscosity relationship for leucogranites, and comparison with synthetic silicic liquids. Trans. R. Soc. Edinb. Earth Sci. 95, 59–72.

Withers, A.C., Behrens, H., 1999. Temperature induced changes in the NIR spectra of hydrous albitic and rhyolitic glasses between 300 and 100 K. Phys. Chem. Miner. 27, 119–132.

Xue, X., Kanzaki, M., 2004. Dissolution mechanisms of water in depolymerized silicate melts: constraints from ^{1}H and ^{29}Si NMR spectroscopy and ab initio calculations. Geochim. Cosmochim. Acta 68, 5027–5057.

Yamashita, S., Kitamura, T., Kusakabe, M., 1997. Infrared spectroscopy of hydrous glasses of arc magma compositions. Geochem. J. 31, 169–174.

Yamashita, S., Kitamura, T., Kusakabe, M., 1999. Infrared spectroscopy of hydrous glasses of arc magma compositions. Geochem. J. 31, 169–174.

Zarubin, D.P., 1999. Infrared spectra of hydrogen bonded hydroxyl groups in silicate glasses. A re-interpretation. Phys. Chem. Glasses 40, 182–190.

Zavel'sky, V.O., Bezmen, N.I., Zharikov, V.A., 1998. Water in albite glasses: OH-groups, isolated molecules, and clusters. J. Non-Cryst. Solids 224, 225–231.

Zhang, Y., Stolper, E.M., Wasserburg, G.J., 1991. Diffusion of water in rhyolitic glasses. Geochim. Cosmochim. Acta 55, 441–456.

Zhang, Y., Belcher, R., Ihinger, P.D., Wang, L.P., Xu, Z.J., Newman, S., 1997. New calibration of infrared measurement of dissolved water in rhyolitic glasses. Geochim. Cosmochim. Acta 61, 3089–3100.

Zotov, N., Keppler, H., 1998. The influence of water on the structure of hydrous sodium tetrasilicate glasses. Am. Mineral. 83, 823–834.